Materials Physics and Mechanics 44 (2020) 439-445 Received: August 24, 2020

STRUCTURE AND PROPERTIES OF ARGON-ARC WELDS OF HIGH-STRENGTH STEEL

P.V. Mel'nikov*, G.D. Motovilina, I.G. Karpov, E.I. Khlusova

NRC "Kurchatov Institute" -CRISM "Prometey", 49 Shpalernaya Str., St.-Petersburg, Russia

*e-mail: npk3@crism.ru

Abstract. Hardness, impact toughness, and structure of slot gap welds (TIG) of low alloyed steel with the ensured yield stress of 890 MPa have been investigated. According to obtained results, the considered technological procedure provides equal strength of the weld and base metals as well as appropriate cold resistance.

Keywords: high-strength steel, argon-arc gap welding, hardness, impact toughness, structure, weld metal, heat affected zone

1. Introduction

To make constructions operating under high loads in arctic regions, shipbuilding has a persisting demand for rolled high-strength low alloyed steels with good weldability. Following the requirements of Russian Maritime Register of Shipping, CRISM "Prometey"-NRC "Kurchatov Institute" has developed steel with a guaranteed yield stress of 890 MPa delivered in thickness of up to 50 mm. Constructions of this steel should ensure reliability when working in polar latitudes and, in this regard, the crucial technological stage is welding. Indeed, it is very hard to get high toughness and cold resistance at a melt-like structure of weld metals strongly affected by the thermal cycle, whereas superposition of weld-related residual stresses with external loads can result in excessive tensile stresses near constructional and technological concentrators. Any employed thermal cycle of welding specifically influences all the above-mentioned factors [1,2].

Argon-arc welding (TIG) [3] enables one to comply with particularly strong requirements to welded joints of high-strength steels [4-8] – formation of the weld metal which ensures a combination of yield strength over 800 MPa and impact energy at temperatures of -40°C and below. This is due to the formation of a dispersed structure of the weld metal. To this end, in particular, the slot gap welding is employed that diminishes the metal deposition and hence consumption of welding wire as well as the level of residual stresses [9,10]; note that related deformations, in this case, become linear rather than angular and also diminish residual stresses. The local strengthening due to the slot gap geometry admits an increase of weld joint strength at the minimum weld reinforcement [11].

The present work is aimed to investigate the structure and properties of slot gap weld joints of 50 mm in thickness made by argon-arc welding (TIG) of steel with the yield stress not less than 890 MPa.

2. Methods

When developing a technological procedure for the slot gap welding (TIG) with a tungsten electrode, a scheme of ends preparation, and geometry of weld joints have been selected, the welding parameters determined and the main requirements to the process formulated.

http://dx.doi.org/10.18720/MPM.4432020_15

For the preparation of the slot gap, combs have been previously deposited onto ends of welded details. This expedient is employed to make complete use of the "local strengthening" effect [12] i.e. constraint of a thin soft layer (weld metal) by harder adjacent parts of base metal. As far as the plasticity of steel saves its volume, any plastic tension along the direction of applied stress σ_1 should result in compression of the same layer in transversal directions; hence, as illustrated in Fig. 1, positive reactive stresses σ_2 and σ_3 appear which reduce the equivalent stress and thus necessitate increased σ_1 and P to satisfy the Mises condition of plasticity.

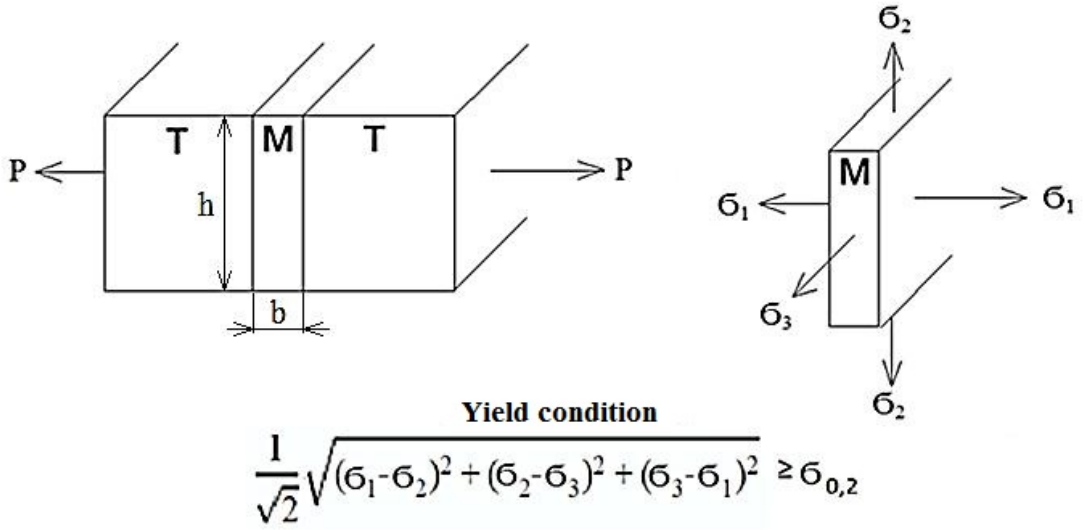

Fig. 1. Scheme of the "local strengthening" in case of slot gap welding where a thin softer layer is constrained by harder surroundings

It is worth noting that to employ advantages of the thin slot gap is rather difficult because the latter complicates manipulations with the welding torch. Accordingly, lack of interrun and side fusion is the most common defect in narrow weld joints. In order to exclude such defects, the welding parameters have been carefully selected by experiments to form proper bead in a slot gap and provide a guaranteed fusion of the welded edges and the previous bead (combs deposited onto ends when root passing). The chemical composition of the steel with yield stress not less than 890 MPa, to be welded, is given in Table 1.

Table 1. Chemical composition of steel

C	Si	Mn	Cr+Mn+Ni+Cu	S	P	V+Nb	CET*
0.09	0.22	1.30	Added	0.0017	0.007	Added	0.37 %

*CET = C + (Mn+ Mo)/10 + (Cu +Cr)/20 + Ni /40

The coupons of 50 mm thick are gap welded with combs deposited onto detail ends were prepared. As widely accepted in Russian shipbuilding for high-strength steels, welding wire Св-07ХН3МД (Sv-07HN3MD) are usually used that provides appropriate physical-mechanical properties of the weld joints made by TIG. The fusion depth has not been measured since in the argon-arc welding this parameter can be reasonably evaluated in terms of 1mm depth per 100 A current [13]. Specific energy input was 2.6 kJ/mm with no preheating of coupons, and inter-pass temperature did not exceed 150°C. General view of the joint is illustrated in Fig. 2 where $b = 12^{+3}$ mm; $l = 20^{+3}_{-1}$ mm; $q = 2^{+2}_{-1}$ mm.

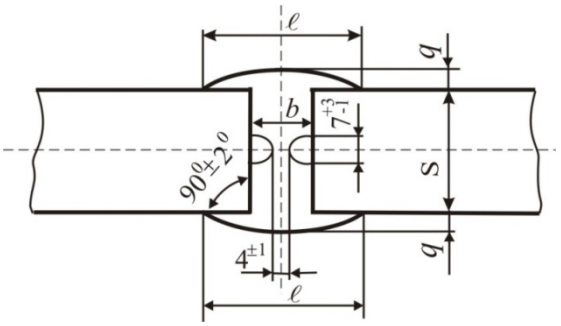

Fig. 2. General view of a joint made by argon-arc welding (TIG)

Templets to measure hardness, specimens for static and impact bending, and metallographic sections have been cut off the weld joint. Vickers hardness is determined at the load of 49 N along lines separated by 2 mm from both joint boundaries and a line situated in the mid-width. Bending tests (tensile stress at the lateral side of the joint) are implemented at a bend former of 40 mm diameter (4 thicknesses of the specimen).

Sharpy specimens were taken 2 mm from the side of the last pass; notches have been introduced after etching the probe and individual marking of specimens in the weld metal, at fusion line, and 2 mm from the latter. The shape and dimensions of the notch were verified by optical microscopy with magnification 30. The testing was performed at 0^oC.

Metallographic analysis of structure with optical microscope Axiovert 40MAT was made on etched sections and fracture surfaces were assessed using scanning electron microscope ResEM 535.

3. Results

A typical weld joint is shown in Fig. 3a consists of 20 layers, each made by two partly overlapping passes. According to this picture, combs are completely remelted, the fusion line is appropriately straight, bead dimensions are stable, and there are no visible defects.

When tested by static bending (tensile load at a lateral weld side) with the required angle of 120 degrees, none of the samples contains any visible defects on the stretched surface (Fig. 3b), that confirms high deformability of trial weld joints. The determined hardness distribution is shown in Fig. 4a-c and Fig. 4d represents the impact toughness of weld joints.

a b

Fig. 3. General view of a weld joint (a) and of its statically bent sample (b)

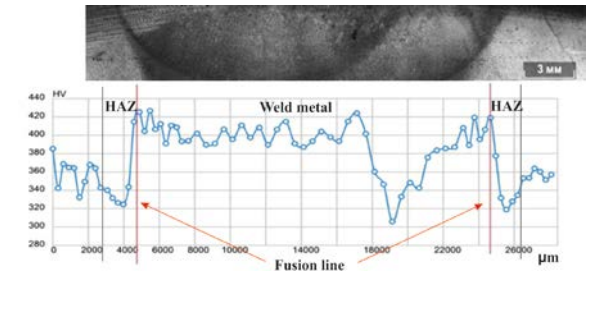

a

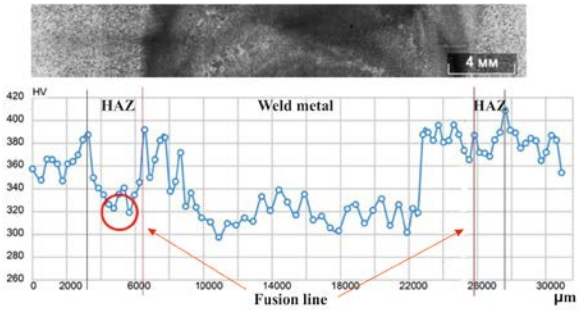

b

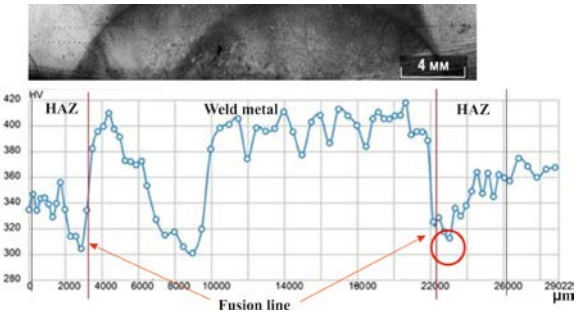

c

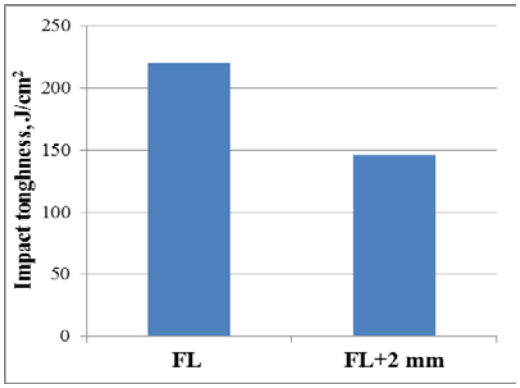

d

Fig. 4. The hardness of weld joint of 500 mm thickness at a distance of 2 mm from the upper side (a), at the mid-line (b), and 2 mm from the lower side (c); impact toughness at 0°C (d), where mean values are given for the fusion line (FL) and at a distance of 2 mm from the fusion line (FL+2mm)

The microstructure of weld metal in the region of extended dendrites is mostly a mixture of martensite and lath bainite; a fraction of granular bainite does not exceed 20% and no ferrite is detected, Fig. 5a-c. This phase composition is predetermined by a high carbon equivalent of weld wear [14,15].

A sharp decrease of hardness in the weld metal shown in Fig. 4 may be due to features of melt (dendritic) structure, as well as chemical non-uniformity and voids on its interfaces. In the mid-thickness of weld metal, a fraction of more than 50% comprises superimpositions and HAZ volumes of beads, Fig. 5c. Annealing or tempering of such domains [16] forms structures of tempered bainite which have lower hardness (Fig. 4 b).

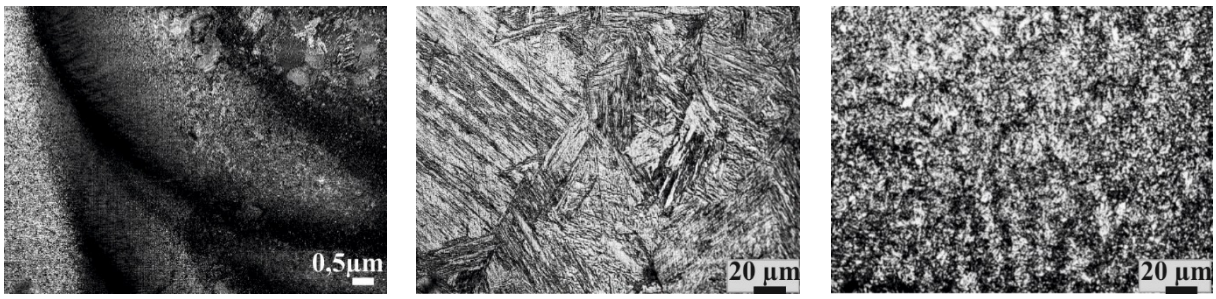

a b c

Fig. 5. Investigated weld joint: general appearance (a), weld meatal structure in the area of extended dendrites (b) and the area of superpositions and HAZ of beads (c)

Analysis of various domains of heat-affected zones (HAZ) of joints brings the following results. The overheated coarse-grained region (CGHAZ) adjacent to the fusion line has a structure of lath martensite transformed from coarse-grained (120 to 150 μm) austenite, Fig. 6a, and hardness close to that of dendritic structure in the weld metal. The size of this region is 300 to 400 μm. In the fine-grained area (FGHAZ) of HAZ extending over about 500 μm bainitic domains are observed in addition to martensite; dimensions of related domains vary from 70 to 20 μm when going from the fusion line, Fig. 6b, where hardness is decreasing.

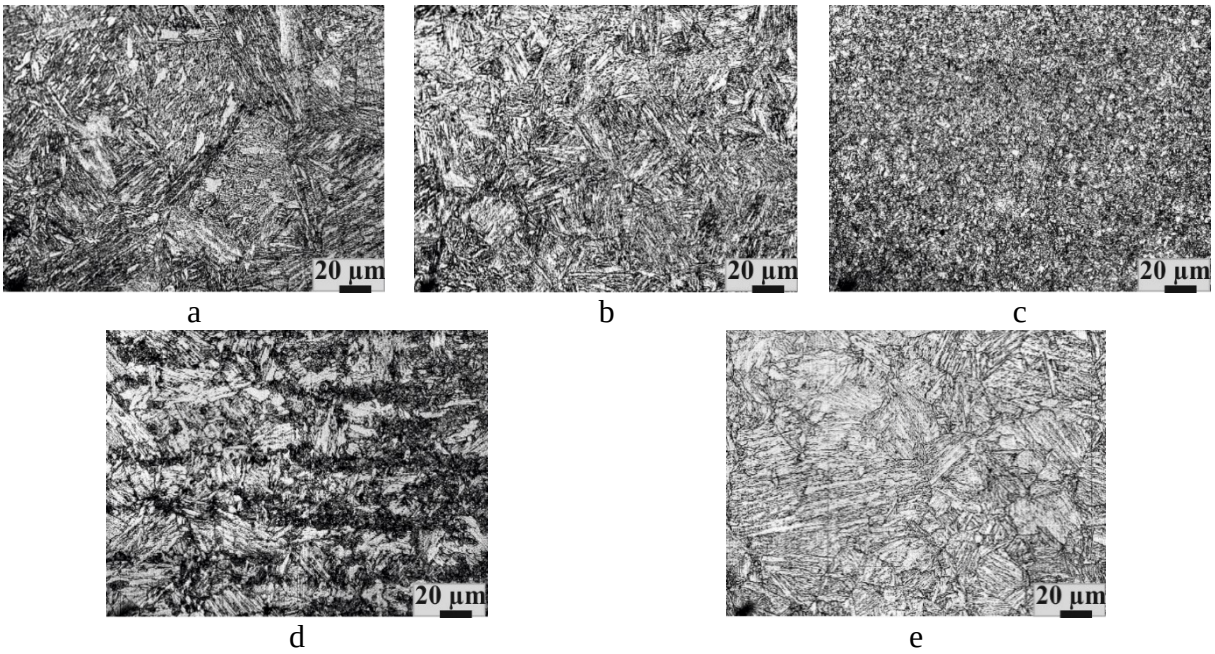

Fig. 6. Structures of HAZ regions: CGHAZ at the fusion line (a), FGHAZ (b), inter-critical ICHAZ (c), sub-critical SCHAZ with enhanced carbide formation (d), and base metal (e)

The third region (ICHAZ) of 2 to 3 mm size (Fig. 6c) forms after heating at inter-critical temperatures and has no distinct interfaces. ICHAZ is made of tempered granular bainite whose element dimensions vary in the range 1 to 10 μm. Usually, hardness within this region is notably lower than in the previously considered ones [17].

Another region extending over 300-500 μm is peculiar in pronounced carbide formation corresponding to the heat removal direction in welding (Fig. 6d) and hardness increasing up to the level of base metal. In the multi-pass welding dimensions of this and previous (third) regions depend on the coordination of neighboring beads. Next, a typical bainitic-martensitic structure of the base metal [18] is represented in Fig. 6e.

According to Fig. 4d, mean values of impact toughness at the fusion line (near the base metal) and 2 mm from the latter are 220 and 146 J/cm^2, respectively. The corresponding fracture surfaces of Sharpy specimens are shown in Fig. 7.

When the notch is situated at the fusion line, Fig. 7a, ductile inter-granular fracture took place assisted by cleavage areas and delamination at interfaces of weld metal. Fig. 7b represents a ductile in-grain fracture in CGHAZ that occupies not more than 10% of the fracture surface.

In case of the notch remoted by 2 mm from the fusion line, the fracture surface contains a mixture of ductile trans- and inter-crystalline fracture in ICHAZ of dispersing bainite (Fig. 7c) and ductile dimple fracture of in-grain character in SCHAZ with the enhanced

formation of carbides, Fig. 7d. No embrittlement signs are found on the fracture surface whereas transitions between fracture types are rather smooth that provides appropriately high toughness of these two zones of HAZ.

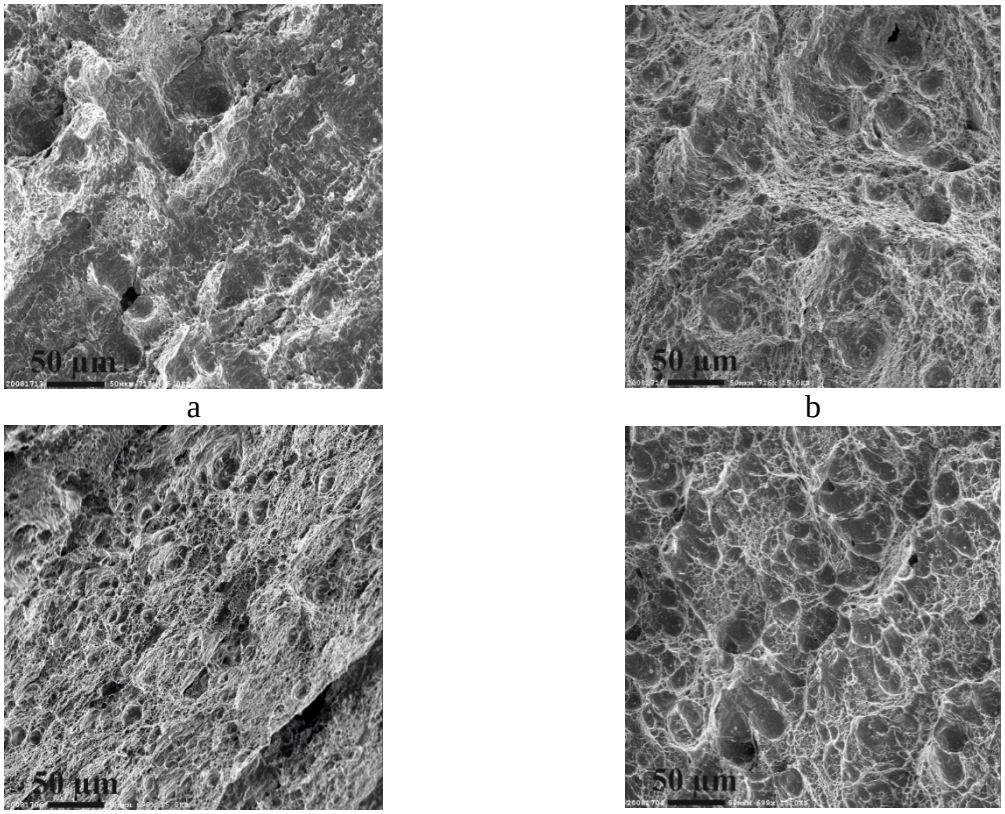

a b c d

Fig. 7. Fracture surfaces of Sharpy specimens with notches at the fusion line (a, b) and 2 mm from the latter (c, d)

To sum up, the microstructure of weld metal and HAZ as well as the fracture character evidence for equal strength levels [19] of weld metal, fusion line, and HAZ of weld joints.

4. Conclusions

The investigated low carbon steel with an ensured yield stress of 890 MPa displayed uniform strength and good cold-resistance of its weld joints. This result, verified by mechanical testing and structure analysis in various domains of the joints, enabled the authors to recommend optimum parameters of argon-arc slot gap welding (TIG) of this perspective material.

Acknowledgements. *The research is supported by the government contract with the code "Arctic steel-2", program "Development of shipbuilding science", Russian Federation national program "Development of shipbuilding and engineering for development of offshore deposits for period of 2013-2030".*

References

[1] Shi Y, Han Z. Effect of weld thermal cycle on microstructure and fracture toughness of simulated heat-affected zone for a 800 MPa grade high strength low alloy steel. *Journal of Materials Processing and Technology*. 2008;207(1-3): 30-39.

[2] Caspar M. Effect of welding heat input on simulated HAZ areas in S960QL high strength steel. *Metals*. 2019;9(11): 1226.

[3] Kristiansen M, Kristiansen E, Jensen CH, Christinsen RH. Vision of arc for quality documentation and for closed loop control of the welding process. *Journal of Automation and Control Engineering*. 2014;2(4): 410-416.
[4] Braun M, Scheffer R, Fricke W, Ehlers S. Fatigue strength of fillet welded joints at subzero temperatures. *Fatigue & Fracture of engineering materials & structures,* 2020;43(2): 403-416.
[5] Kornél M, Borók A, Pasquale RS, Varbai B. TIG welding of advanced high strength steel sheets. In: *Proc. International scientific conference on advances in mechanical engineering.* Debrecen, Hungary; 2016.
[6] Lukács J, Dobosy Á, Gáspár M. Fatigue Crack Propagation Limit Curves for S690QL and S960M High Strength Steels and their Welded Joints. *Advanced Materials Research*. 2018;1146: 44-56.
[7] Aymetov SF, Aymetov FG. The strength of butt joints weakened by soft interlayer under bending load. *Bulletin of the South Ural State University*. 2015;15(1): 107-112.
[8] Shakhmatov DM. Bearing capacity of joints mild interlayer flexural. *The Modern Challenges in Science and Education.* 2014;2: 48.
[9] Balakshan J, Vasileiou AN, Francis JA, Smith MC, Roy MJ, Callaghan MD, Irvine NM. Residual stresses distribution in arc, laser and electron-beam welds in 30 mm thick SA508 steel: A cross process comparison. *International Journal of Pressure Vessels and Piping*. 2018;162: 59-70.
[10] Francis JA, Vasileiou AN, Roy MJ, English PD, Balakshan J, Smith MC, Callaghan MD, Irvine NM. Residual stresses in arc and electron beam welds in 130 mm thick SA508 steel: Part 1- manufacture. *International Journal of Pressure Vessels and Piping.* 2019;172: 313-328.
[11] Bakshi OA, Shatov AA. On the stress state and deformation of solid metal in welded joints comprising a hard soft interlayers. *Svarochnoe Proizvodstvo*.1966;5: 7-10. (In Russian)
[12] Bakshi OA. On the stress state of soft interlayers in welded joints at tension (compression). In: *Voprosy svarochnogo proizvodstva*. Chelyabinsk: ChPI; 1965. (In Russian)
[13] Muller VV. The Influence of Mode Parameters of Argon-Arc Welding Performed by Nonconsumable Electrodes on the Fusing Depth. In: *Collected articles for the 7th Science Conference "Perspectives of Science Development in the Modern World"*. Ufa; 2018. p.88-89.
[14] DiX, Tong M, Li C, Zhao C, Wang D. Microstructural evolution and its influence on toughness in simulated intercritical heat affected zone of large thickness bainitic steel. *Materials Science & Engineering.* 2019;A743: 67-76.
[15] Lambert-Perlade A, Gourgues AF, Pineau A. Austenite to bainite phase transformation in the heat-affected zoneof a high strength low alloy steel. *Acta Materialia*. 2004;52(8): 2337-2348.
[16] Yu X, Caron JL, Babu SS, Lippold JC, Isheim D, Seidman DN. Strength recovery of a high-strength steel during multiple weld thermal simulation. *Metallurgical and Materials Transaction*. 2011;A42: 3669-3679.
[17] Yoo J, Kim S, Park Y, Lee C. Evaluation of Mechanical Properties in Heat Affected Zones of Fe-8Mn-0.06C Steel Welds. In: *Proceedings of International Conference on Advanced Steels 2010*. Contributed Papers Beijing; 2010.
[18] Zisman AA, Zolotorevsky NY, Petrov SN, Khlusova EI, Yashina EA. Panoramic crystallographic analysis of structure evolution in low-carbon martensitic steel under tempering. *Metal Science and Heat Treatment*. 2018;60: 142-149.
[19] Minami F, Toyoda M, Thaulow C, Hauge M. Effect of strength mis-match on frature mechanical behavior of HAZ-notched weld joint. *Quaterly Journal of the Japan Welding Society*. 1995;13: 508-517.